JOURNAL OF GEOPHYSICAL RESEARCH, VOL. 96, NO. D2, PAGES 2897–2912, FEBRUARY 20, 1991

STRATOSPHERIC CLOUD OBSERVATIONS DURING FORMATION OF THE ANTARCTIC OZONE HOLE IN 1989

D. J. Hofmann and T. Deshler

Department of Physics and Astronomy, University of Wyoming, Laramie

Abstract. The results of six balloon flights at McMurdo Station, Antarctica, under varying temperature conditions, are used in a study of polar stratospheric clouds during September 1989. A new particle counter, with size resolution in the 0.5 μm radius region, indicated that size distributions observed in the clouds were bimodal. Mode radii ranging from 0.05 to 0.10 μm were observed for the small particle mode, representing the sulfate layer or condensational growth enhancements of it. Mode radii generally ranged from 1.5 to 3.5 μm for the large particle mode at concentrations 3 to 4 orders of magnitude lower than the small particle mode. The large particle mode, when observed at temperatures above the water ice point, is believed to be the result of nitric acid trihydrate (NAT) condensation on larger particles of the sulfate layer. In this case the HNO_3 condensed mass mixing ratios were 1 to 5 ppbv for most of the cloud layers. Generally, the large particle NAT concentrations were higher in the lower stratosphere, indicating the redistribution of HNO_3 through particle sedimentation. On several occasions, distributions were observed with mode radii as high as 7 μm, and correspondingly large inferred mass, indicating water ice clouds in the 12 to 15 km region. On other occasions, absence of such clouds at very low temperatures inferred water vapor mixing ratios of less than 3 ppmv.

Introduction

The presence of clouds in the stratosphere is now generally accepted as a prerequisite for the heterogeneous chemical preconditioning of chlorine-bearing molecules necessary for the destruction of stratospheric ozone in the Antarctic spring (see Solomon [1988] for a review of the related chemistry). These clouds are believed to be composed primarily of either NAT or water, depending on the temperature [Toon et al., 1986; Crutzen and Arnold, 1986]. Depending on H_2O and HNO_3 concentrations, NAT condensation is expected to occur at 3°-7° C warmer than for water ice clouds [Hanson and Mauersberger, 1988]. Measurements to date in the Antarctic [Fahey et al., 1989; Gandrud et al., 1989; Hofmann et al., 1989a; Pueschel et al., 1989] and in the Arctic [Hofmann et al., 1989b; Hofmann and Deshler, 1989; Kawa et al., 1990; Gandrud et al., 1990; Kondo et al., 1990; Pueschel et al., 1990] are generally in agreement with this hypothesis although the details of the particle formation processes and particle size distributions are not well known.

Although a greater wealth of knowledge is gained by simultaneously observing all components of the particle formation process, i.e., pressure, temperature, particle size distribution, and H_2O and HNO_3 concentration, the temperature history of the air parcel is also important since the number of condensation nuclei (CN) taking part in the condensational process depends on the degree of vapor supersaturation and thus on the temperature history. In addition, the rate of cooling becomes important in determining the eventual particle size. Fast cooling uses up the available vapor rapidly and limits particle size since more of the CN take part in the growth process, while slow cooling appears to result in only the largest ($r > 0.3\ \mu$m) particles in the sulfate layer growing, thus resulting in larger NAT particles. Combinations of these processes can result in multimodal particle size distributions [Hofmann et al., 1989a]. Thus it is generally very difficult to study the particle formation and growth process in any detail, and for the moment, efforts are limited to either studying most of the aspects at limited opportunities and in limited height ranges, such as studies utilizing high altitude aircraft as in the Airborne Antarctic and Arctic Expeditions [Tuck et al., 1989; Turco et al., 1990], or by studying limited aspects at more frequent intervals and larger height ranges, i.e., attempting to develop a climatology of polar stratospheric cloud (PSC) properties. Using satellites to monitor solar extinction caused by PSC formation [McCormick et al., 1989] is an example. We here report on a continuing effort in the latter category, namely to measure the PSC particle size distributions under various temperature conditions using balloonborne particle counters.

Paper number 90JD02494.
0148-0227/91/90JD-02494$05.00

Instrumentation

Measurements in Antarctica during 1986 and 1987 (NOZE I and II) were made with an optical particle counter which measured scattered white light at 25±5° from the forward scattering direction with a flow rate of about 1 L min^{-1} [Hofmann et al., 1988, 1989a]. This is the standard "dustsonde," which measures particles having r ≥ 0.15 and 0.25 μm, used for many years at Laramie, Wyoming, to study the stratospheric sulfate layer [Hofmann et al., 1975], but with added size channels for large (r ≥ 1 μm) particles. Although the flow rate was barely adequate to detect low concentration (< 10^{-2} cm^{-3}) PSC particles, it was sufficient to determine, at McMurdo (78° S) in the very cold spring of 1987, that for stratospheric temperatures less than about -79° C, the aerosol size distribution in the sulfate layer was bimodal. The large particle mode appeared to result from NAT condensation on sulfate aerosol having radii greater than about 0.3 μm [Hofmann et al., 1989a]; however, size resolution was not adequate to clearly characterize the large particle mode.

In order to further study this observation a high flow rate (12 L min^{-1}) optical counter measuring at 27±5° was developed for PSC measurements in 1988. This instrument improved the lower concentration limit to about 10^{-3} cm^{-3}. In addition, questions about possible evaporation of the particles in the ≈10-cm inlet, operated at about 10° C, were addressed by keeping the inlet tube near ambient temperature. Although the 1988 spring stratosphere at McMurdo was not very cold, the new instrument was used to detect particle-ozone correlations in PSCs [Hofmann, 1989]. Both of these instruments, however, suffered from a double-valued response in the region where the particle size was similar to the wavelength of the scattered light, i.e., radii of about 0.5 μm [Hofmann et al., 1989a]. This precluded size discrimination in the 0.3 to 1.0-μm radius range, a region critical for NAT studies since models suggested that the NAT particles formed should be in this size range [Toon et al., 1986; Poole and McCormick, 1988a]. To remove the ambiguities in the 0.3 to 1.0 μm region, the scattering angle was increased to 40°. This decreased the amount of scattered light for large particles by about a factor of 2, but increased the relative response near 0.5 μm, and removed the double-valued response. Figure 1 compares the calculated response (phototube pulse height versus particle radius) of a 27° and 40° particle counter for a typical midlatitude stratospheric sulfuric acid - water aerosol and for NAT in solution form, assuming spherical particles. The improved response is clear in Figure 1. Tests at Laramie in the summer of 1989 with this instrument indicated that for the first time we could resolve 0.5 μm radius particles, both in the stratospheric sulfate layer and in cirrus clouds.

Figure 2a shows the 40° calculated counter

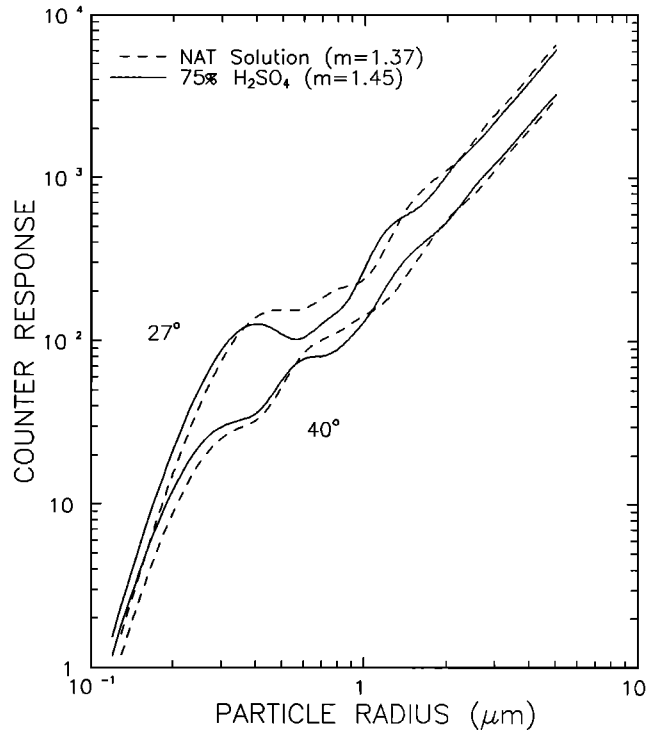

Fig. 1. Optical particle counter response curves (phototube pulse height versus particle size) for two different scattering angles and two different indices of refraction (particle compositions).

response and measurements using calibrated polystyrene aerosol. The relative minimum in the measured response for polystyrene at about 0.5 μm radius, a prominent feature of the 25° counters [Hofmann et al., 1989a], is greatly reduced as expected from the response calculations. Figure 2b shows the calculated response for those particle indices of refraction which are likely to be encountered in the polar stratosphere, including NAT crystals, which may have an index of refraction of 1.51 [Toon et al., 1990]. Except for the latter, the response curves are single valued and similar for water, NAT solution (or amorphous form), and 40% sulfuric acid, a value expected at -85° C [Steele and Hamill, 1981]. The physical form of NAT in the stratosphere is not known. Laser backscatter polarization measurements suggest that particles encountered at temperatures warmer than the water ice point are nearly spherical [Poole and McCormick, 1988b] although slightly aspherical, crystalline NAT particles may be present at times [Rosen et al., 1989; Browell et al., 1990]. Temperature history may dictate which physical state forms.

Size discrimination levels were set at 0.15, 0.25, 0.50, 1.0, 2.0, 3.0, and 5.0 μm radius, thus avoiding the regions of flat response between 0.25 and 0.4 μm radius and between 0.5 and 0.7 μm radius for a possible NAT crystalline particle composition (see Figure 2b). Aside from statistical uncertainties which arise when concen-

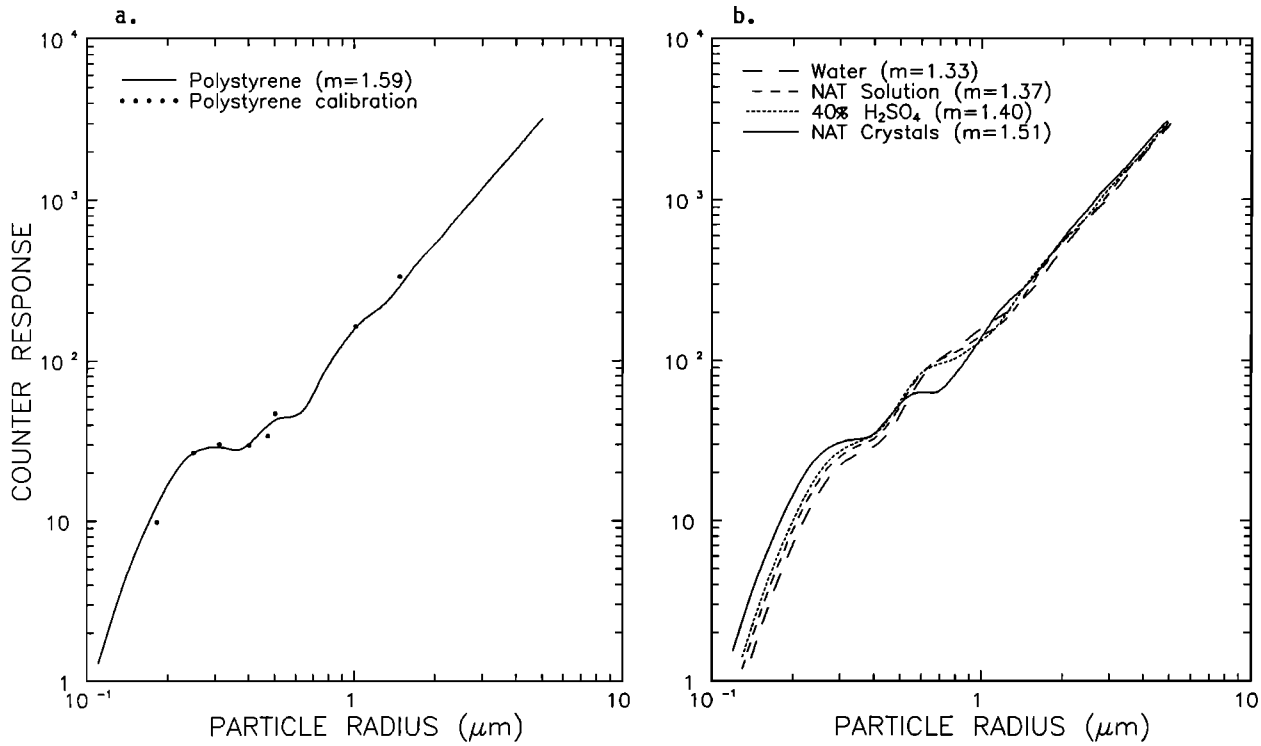

Fig. 2. Optical particle counter response curves (phototube pulse height versus particle size) (a) for polystyrene aerosol compared to measured points, and (b) for several indices of refraction (particle composition) of interest in polar stratospheric clouds, for the 40° scattering angle counter.

trations are less than about 10^{-2} cm^{-3} (depending on the altitude averaging interval), the sizing accuracy for spherical particles is estimated to be about 10% which translates into a mass uncertainty of about 30%. The sizing error for large, nonspherical particles is unknown but could result in a large mass estimate error. These counters were flown successfully during the austral spring of 1989 at McMurdo on five occasions, four of which encountered PSCs. In addition, for a baseline comparison a standard dustsonde was flown after temperatures had increased in October. Also, condensation nuclei counters, utilizing thermal growth chambers and optical particle counters [Hofmann et al., 1989a], were flown on four occasions to determine the total aerosol concentration or total number of condensation sites. The aerosol data collected during these flights are the subject of this paper.

Observations

As reported earlier [Deshler et al., 1990], the spring of 1989 was as severe as 1987 in terms of ozone depletion and temperature minima although the low temperatures did not last as long in 1989. The 18±1 km temperatures and ozone mixing ratios are shown in Figure 3 for reference. The six balloon flights carrying aerosol size-discriminating instruments were conducted between September 3 and October 16, a period during which the ozone depletion process was underway.

Figure 4 shows vertical profiles of condensation nuclei (CN) measured during the PSC observations

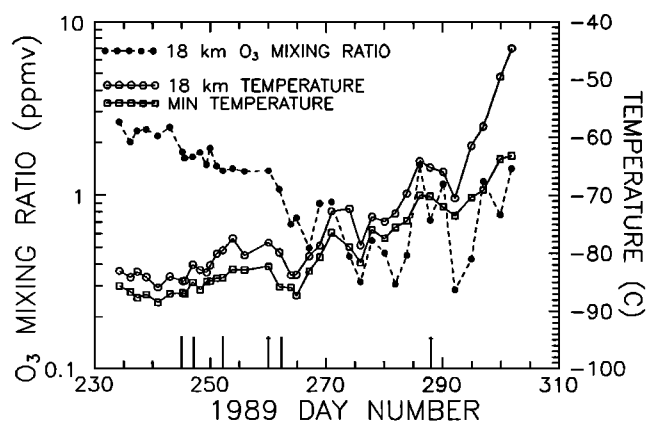

Fig. 3. Temperature and ozone mixing ratio versus time at 18±1 km measured at McMurdo Station, Antarctica, during the spring of 1989. The minimum temperature measured during each sounding is also shown. The times of the particle counter flights discussed here are indicated by arrows.

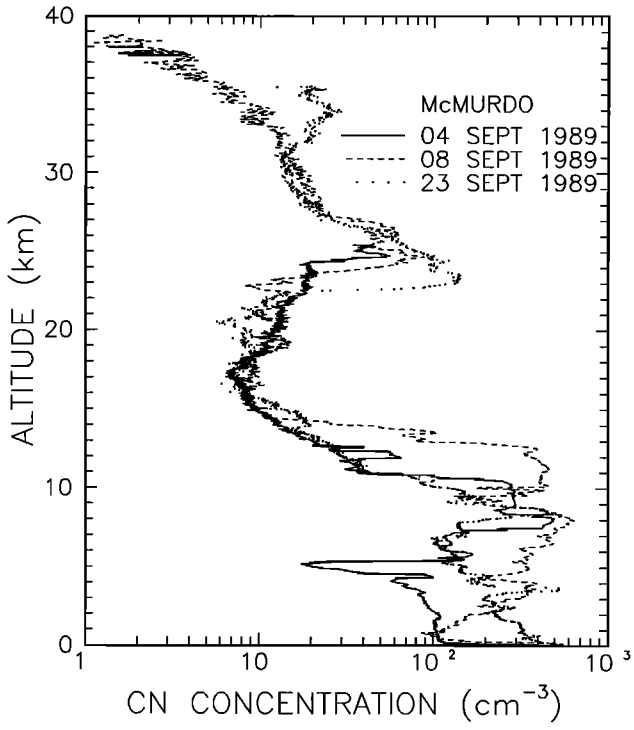

Fig. 4. Condensation nuclei profiles measured at McMurdo Station, Antarctica, during the spring of 1989.

reported here. These data represent the total aerosol ($r \geq 0.01$ μm) concentration and are important in normalizing size distributions measured at larger sizes. They are also important in PSC formation as they represent the total number of condensation sites. In the PSC formation region (10 to 22 km), the total aerosol concentration remains relatively constant, lacking the sources present in the troposphere and at high altitude. High concentrations of CN at high altitude are related to nucleation of sulfuric acid vapor in the cold Antarctic winter upper stratosphere [Hofmann et al., 1988; 1989a], while the layer of enhanced CN in the 22 to 26 km region is believed to be of photochemical origin [Hofmann, 1990a]. Since this region is generally above the PSC formation region, these elevated levels of CN are not relevant to the study here.

Sulfate Layer Deliquescence

It has long been realized that as the stratospheric sulfate (sulfuric acid - water aerosol) layer cools in the early Antarctic winter, the supercooled liquid droplets will take on water (deliquesce) and swell in size. This process was believed to continue until the droplets freeze forming ice crystals at about -85° C, for a typical H_2O mixing ratio of 5 ppmv at 20 km [Steele et al., 1983]; however, it is now believed that before the ice crystal stage is reached, NAT condensation occurs, at a temperature of about -80° C for typical H_2O and HNO_3 mixing ratios (5 ppmv and 10 ppbv at 20 km, respectively) [Toon et al., 1986; Crutzen and Arnold, 1986]. The condensational growth of NAT may thus substantially mask the deliquescence process so that it can probably only be observed during the initial cooling process in the Antarctic winter, in the spring at stratospheric warming, or under conditions of severe denitrification as occurred in 1987 [Fahey et al., 1989]. During the particle counter flights in 1989, temperatures in the sulfate layer (12 to 16 km) were generally between -75° C and -79° C, except on September 20 when they were about -82° C and during the final background flight on October 16 when they were about -68° C. Thus the conditions necessary for detecting deliquescence may have been present.

Figure 5 shows the temperature, $r \geq 0.15$ and $r \geq 0.25$ μm concentration profiles for the six particle counter balloon flights which took place between September 3 and October 16. Compared to the background sounding with a standard dustsonde on October 16, enhancements in the region of the sulfate layer (12 to 16 km) appear to exist in both particle size ranges except possibly on September 10 when temperatures in this region only reached about -75° C. On September 3, 5, and 20, particle enhancements extended to altitudes above 18 km. Temperatures on these soundings reached the NAT condensation point resulting in the formation of large particles as will be discussed later. The sounding on September 20 shows even larger enhancements in the middle of the sulfate layer in a region which was about 5° colder than the previous soundings (about -83° C at 13 to 14 km) so that deliquescence would clearly be masked in this case.

Ideally, to detect deliquescence, following an air parcel as it cools is required. Comparisons of concentration profiles at different times can be somewhat misleading even if NAT condensational effects are absent, although the general variability of the sulfate layer is not large [Hofmann et al., 1989a]. Since the sulfate layer average particle size is not expected to vary as much as the concentration, and since deliquescence results in generally larger particles, it may be more fruitful to investigate changes in particle size. Figure 6 shows the six aerosol profiles in terms of the size ratio R the ratio of the $r \geq 0.15$ μm concentration to the $r \geq 0.25$ μm concentration. This ratio has typically had a value of 3 to 4 in the region of the sulfate layer under undisturbed conditions. Both deliquescence and NAT growth should result in a decrease in R. As indicated in Figure 6, the largest particles (smallest ratio) occurs in the sulfate layer between 12 and 16 km but there is no clear decrease in R with average temperature in this region. This could be due to different temperature histories of the air parcels.

To determine the degree of change in R that might

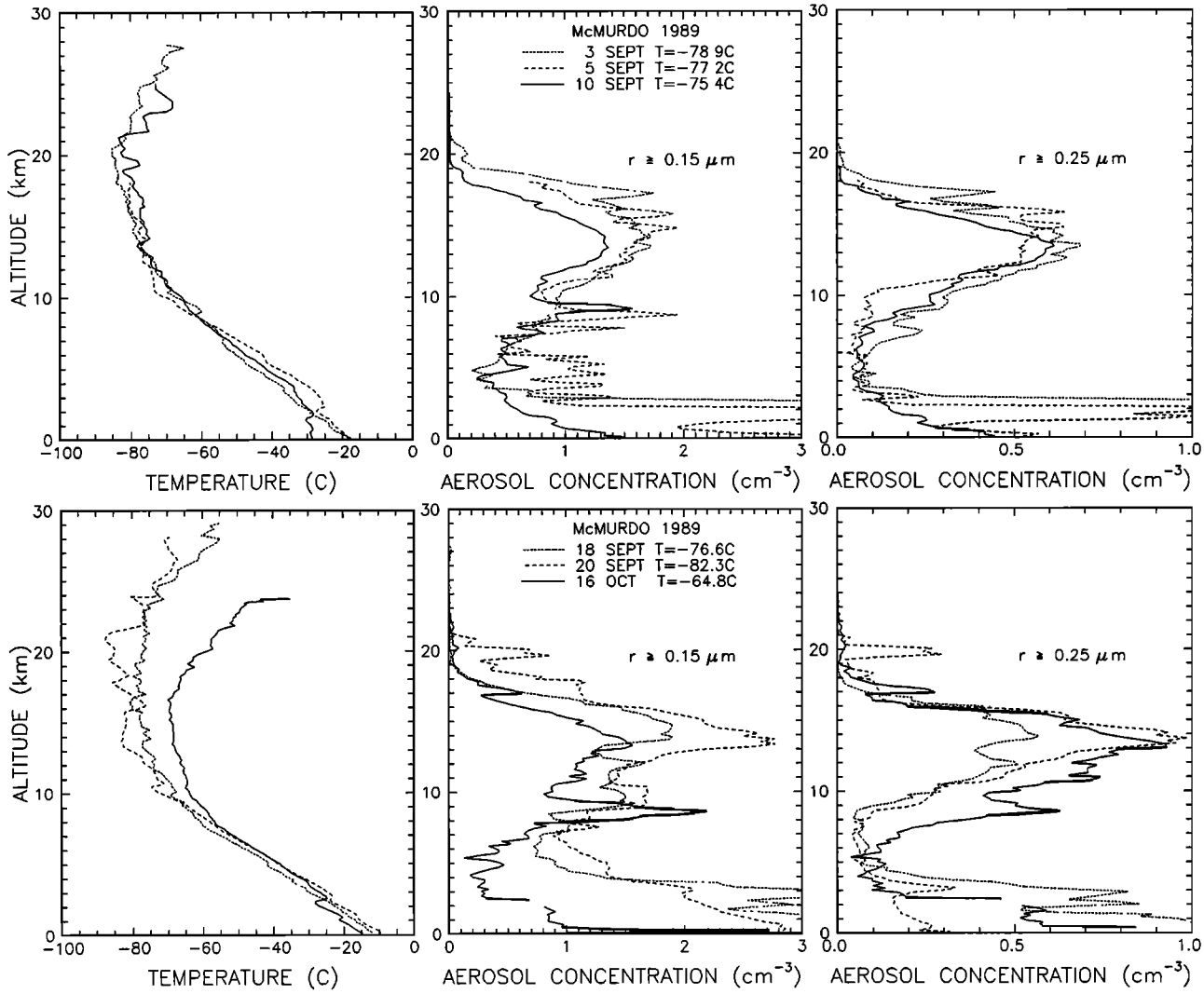

Fig. 5. Temperature, r ≥ 0.15 μm, and r ≥ 0.25 μm aerosol concentration profiles measured at McMurdo Station, Antarctica, during the spring of 1989.

be expected for a given temperature change, the size distribution must be parameterized. As will be discussed in more detail later when PSC size distributions are presented, stratospheric aerosol size distributions are best represented by the lognormal distribution. However, for a limited size range involving radii greater than the mode radius, r_0, an exponential distribution is adequate. For a differential distribution, $n(r) = n_0 \exp(-r/r_0)$, and for the size ratio, $R = N(\geq 0.15)/N(\geq 0.25)$, the fractional change in R for a change in mode radius is given by $dR/R = -(\ln R)dr_0/r_0$.

Steele and Hamill [1981] have investigated the change in size of the stratospheric sulfuric acid aerosol for changes in temperature and water vapor content. If we use their results and assume that a change in r will be reflected in a change in r_0, then we may estimate the change in R as temperature changes. The results are given in Figure 7 for two cases, a change from -85° C to -80° C, involving a theoretical change in r of -13%, and for -80° C to -75° C, involving a theoretical change in r of -6%. Only the latter case is probably of interest as the former would be dominated by NAT condensation except under conditions of severe denitrification. The change in R, as indicated in Figure 7, is of magnitude similar to the change in r for the mode radii or size ratios encountered ($R \approx 3$) in the sulfate layer. Thus, for the situations in which we might be able to detect deliquescence, i.e., when temperatures have warmed from about -80° C to -75° C, we may expect only about a 6% change in the size ratio. Figure 8 shows R as a function of temperature both for measured 2 km intervals at 12, 14, and 16 km, and as predicted by theory for warming from an initial condition of a ratio of 3 at -85° C. While the observed variation in R is not inconsistent with the occurrence of deliquescence, large fluctuations in the observed value of R, possibly due to NAT

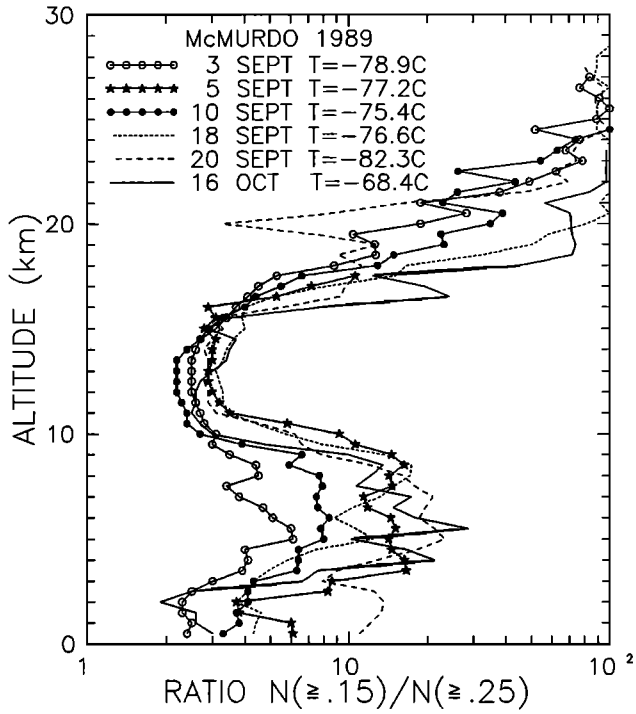

Fig. 6. The ratio of r ≥ 0.15 μm to r ≥ 0.25 μm aerosol concentration as a function of altitude at McMurdo Station, Antarctica, during the spring of 1989.

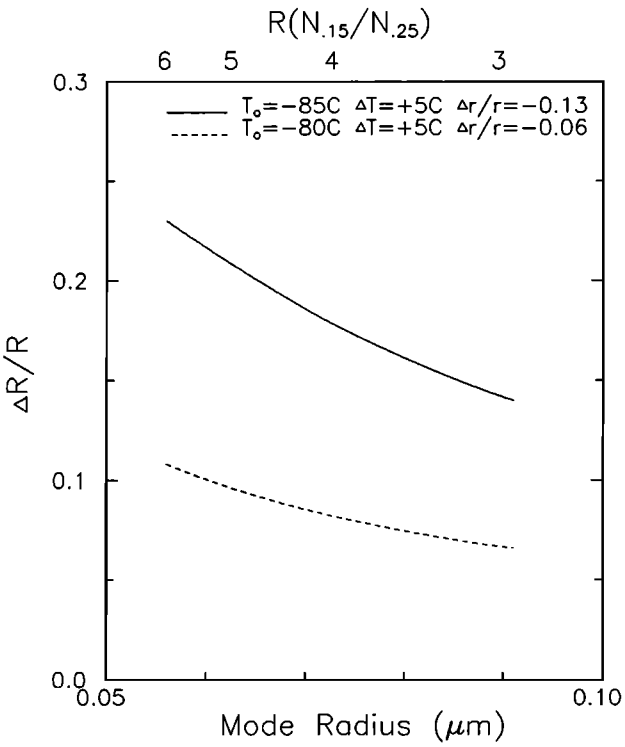

Fig. 7. Theoretical variation of the ratio of r ≥ 0.15 μm to r ≥ 0.25 μm aerosol concentrations for a warming of 5° C from -85° C and -80° C as a function of aerosol size distribution mode radius.

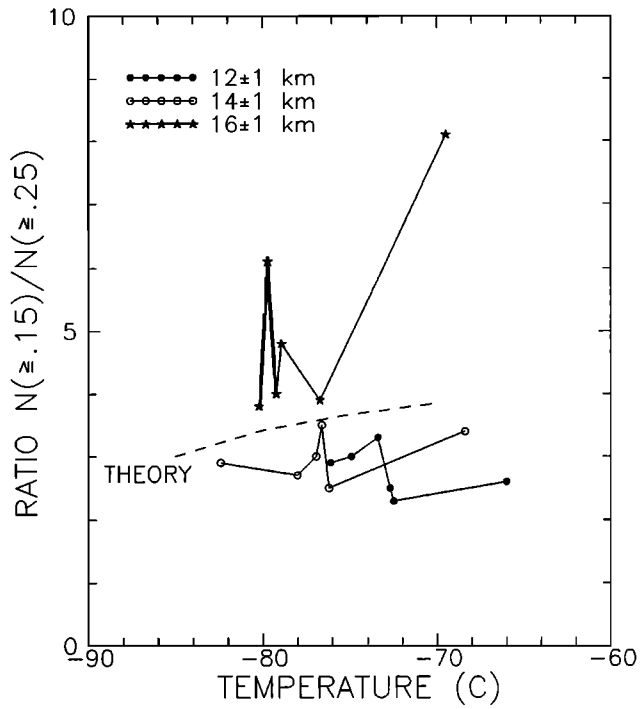

Fig. 8. Observations of the variation of the ratio of r ≥ 0.15 μm to r ≥ 0.25 μm aerosol concentrations as a

condensation near temperatures of -80° C and general variability above this temperature, preclude clear detection of deliquescence by this technique.

PSC Size Distributions

In this section we present height profiles of temperature and particle concentration, and the PSC particle size distributions, for the five soundings using the high flow rate counter. In the ensuing discussion, knowledge of water vapor and nitric acid vapor mixing ratios would greatly aid in the interpretation of the data. Lacking such measurements, we refer to previous situations under similar conditions as a guideline. By mid to late August in 1987, a year of similar temperatures and ozone depletion, water vapor mixing ratios were about 3 ppmv [Rosen et al., 1988; Kelly et al., 1989]. Ice cloud formation and precipitation had caused dehydration during the Antarctic winter which reduced the water vapor mixing ratio from the normal prewinter value of about 5 ppmv. It is thus likely that water vapor mixing ratios were closer to 3 ppmv than 5 ppmv in September of 1989. Similarly, values of nitric acid vapor mixing ratio well below the prewinter value of about 10 ppbv were inferred from simultaneous NO_y and particle observations, from aircraft in Antarctica in 1987, indicating substantial denitrification had occurred [Fahey et al., 1989]. However, these inferred nitric acid mixing ratios did not appear to be as uniformly low as in the

case of water vapor. We thus might expect values to vary over the range of 2 to 10 ppbv.

The particle size distributions will be described in terms of a lognormal distribution. Such a distribution may be written in differential form as

$$n(r)dr = \frac{N_0}{(2\pi)^{1/2}} \exp(-\frac{\alpha^2}{2})d\alpha$$

where $$\alpha = \frac{\ln(r/r_0)}{\ln\sigma}$$

The single mode lognormal distribution involves three parameters, the total number concentration (or mixing ratio), N_0, the distribution median radius, r_0, (one half of the particles have radii greater than or less than r_0), and the distribution width, σ. Typical values for the current background stratospheric aerosol layer as measured at Laramie (41° N) are $N_0 = 6$ cm^{-3}, $r_0 = 0.04$ μm, and $\sigma = 2.5$ ($\sigma = 1$ corresponds to a monodispersed aerosol) [Hofmann, 1990b]. The integral size distribution, which is measured in this work, is given by

$$N(\geq r) = \int_r^\infty n(r')dr'$$

Since the size distribution involves three parameters, a measurement of the concentration at a minimum of three sizes is required. Thus a measurement of the total aerosol concentration N_0 with a condensation nuclei counter and the two integral ranges $N(\geq 0.15)$ and $N(\geq 0.25)$ are sufficient to determine the parameters of a single-mode lognormal size distribution. While this technique is adequate for the normal sulfate layer, the large particle component in a PSC forms an additional mode, requiring three more independent measurements. Since we generally have five more (concentration at $r \geq 0.5$, 1, 2, 3, and 5 μm, although $r \geq 5$ μm particles are not always present), a method has been developed to select the most useful concentrations to obtain the best fit in a least squares sense to the second mode.

The total aerosol mass concentration (or mixing ratio) for spherical particles in a given lognormal mode is

$$M = \frac{4}{3}\pi D N_0 r_0^3 \exp[\frac{9}{2}(\ln\sigma)^2]$$

where D is the aerosol specific gravity (1.65 g cm^{-3} for 75% H_2SO_4, 25 % H_2O; 1.62 g cm^{-3} for NAT).

The total particle surface area concentration for spherical particles in a given lognormal mode is

$$A = 4\pi N_0 r_0^2 \exp[2(\ln\sigma)^2]$$

Table 1, which will be referred to in the following discussion, tabulates the bimodal parameters, masses,

TABLE 1. PSC Lognormal Parameters, Mass and Area

Date	Press, hPa	Alt, km	Temp, °C	N_1, cm^{-3}	r_1, μm	σ_1	Area$_1$, μm^{2}cm^{-3}	Mass$_1$, μg m^{-3}	H_2SO_4*, ppbm	HNO_3*, ppbv	N_2, cm^{-3}	r_2, μm	σ_2	Area$_2$, μm^{2}cm^{-3}	Mass$_2$, μg m^{-3}	H_2O*, ppmv	HNO_3*, ppbv
Sept. 3	148	12.5	-73.5	33.0	0.048	2.22	3.38	0.264	1.69	0.41	0.0053	1.92	1.97	0.62	1.26	0.008	1.96
	125	13.5	-77.2	20.0	0.086	1.79	3.65	0.245	1.82	0.44	0.0005	3.51	1.44	0.11	1.83	0.001	0.33
	96	15.0	-79.1	10.0	0.094	1.82	2.26	0.173	1.66	0.40	0.0042	7.65	2.40	1.43	246	2.30	571
	47	19.0	-84.0	11.0	0.057	1.64	0.74	0.026	0.50	0.12	0.0072	1.39	2.03	0.48	0.78	0.015	3.62
Sept. 5	194	11.0	-73.5	49.0	0.026	2.47	2.08	0.138	0.67	0.16	0.0087	2.08	2.01	1.25	2.93	0.014	3.45
	150	12.5	-76.0	33.0	0.034	2.52	2.68	0.260	1.61	0.39	0.0067	1.04	2.53	0.51	1.53	0.009	2.31
	138	13.0	-76.6	23.0	0.053	2.18	2.69	0.215	1.45	0.35	0.0053	2.02	2.07	0.77	1.93	0.013	3.16
	106	14.5	-77.7	14.0	0.084	1.87	2.70	0.201	1.75	0.43	0.0013	3.37	1.62	0.30	0.61	0.051	1.28
	75	16.5	-80.6	8.0	0.091	1.70	1.46	0.090	1.09	0.27	0.0071	2.00	1.53	0.52	0.54	0.006	1.60
Sept. 10	124	13.5	-77.7	20.0	0.079	1.84	3.34	0.225	1.68	0.41							
Sept. 18	175	11.5	-72.6	38.0	0.041	2.20	2.83	0.185	1.00	0.24	0.0046	5.28	1.58	2.44	7.28	0.039	9.58
	124	13.5	-77.2	20.0	0.060	2.07	2.57	0.192	1.43	0.35	0.0132	2.11	1.85	1.58	2.87	0.021	5.20
	81	16.0	-79.5	8.0	0.093	1.79	1.71	0.123	1.40	0.34	0.0029	1.93	1.51	0.19	0.19	0.002	0.53
Sept. 20	178	11.5	-73.8	38.0	0.051	2.06	3.45	0.214	1.13	0.28	0.0014	4.22	1.18	0.33	0.50	0.003	0.65
	126	13.5	-82.7	20.0	0.089	1.85	4.29	0.331	2.38	0.58	0.0006	4.06	1.19	0.14	0.20	0.001	0.35
	105	14.5	-82.3	14.0	0.090	1.91	3.27	0.278	2.40	0.58	0.0025	2.53	1.48	0.27	0.34	0.003	0.70
	88	15.5	-82.1	10.0	0.106	1.74	2.62	0.199	2.06	0.50	0.0019	2.93	1.70	0.34	0.73	0.007	1.82
	39	20.0	-84.9	11.0	0.050	2.23	1.24	0.103	2.32	0.56	0.0003	2.70	1.24	0.03	0.03	0.0007	0.18

*Inferred vapor mixing ratios for the calculated mass concentration.

and areas for a number of PSC layers encountered during the five soundings under discussion.

September 3, 1989. Figure 9 shows the temperature profile and particle concentration profiles for six size ranges between 8 and 22 km observed on September 3. Also given are the temperature versus altitude (pressure) relation for the frost point and NAT condensation, from the data of Hanson and Mauersberger [1988], for applicable ranges of water and nitric acid vapor mixing ratios (3 to 5 ppmv H_2O, 2 to 10 ppbv HNO_3). The temperatures between 13 and 20 km are low enough to condense essentially all available HNO_3 vapor unless the H_2O vapor mixing ratio was substantially below 3 ppmv. The particle data indicate layers of particles with $r \geq 1$ μm between 11 and 22 km. Particles of this size are not observed at these concentration levels in the normal sulfate layer observed on, for example, September 10, 1989 (see Figure 14). Temperatures were not low enough to condense water vapor, for H_2O mixing ratios less than about 5 ppmv, so it is not likely that the enhanced large particles were water ice and thus were more likely composed of NAT.

For a uniform 3 ppmv H_2O mixing ratio profile, the observation of large particles between 12 and 13 km suggests HNO_3 mixing ratios as high as 10 ppbv in this region while a lack of particles between 13 and 14 km would suggest near complete denitrification in this region. This complicated structure could result from layers of HNO_3 depletion owing to previous condensation and precipitation redistributing HNO_3 vapor to the lower stratosphere. Such redistribution of HNO_3 was observed in the Arctic winter of 1989 [Arnold et al., 1989; Hübler et al., 1990; Schlager and Arnold, 1990]. Similarly, it could be caused by nonuniformity in the H_2O profile. Further information on the nitric acid mixing ratio in these regions can be obtained from the mass in the particle distributions as given in Table 1. We see that at 12.5 km the large particle mode has about 2 ppbv of HNO_3 in it for an NAT composition. Thus, although the condensation temperature suggests that at least 10 ppbv was available, only 2 ppbv appears to have condensed when the layer was measured. At 13.5 km, only 0.33 ppbv of HNO_3 is present in the particles, consistent with the premise that this layer may have been highly denitrified, on the assumption that condensational equilibrium had been established.

Figure 10 shows the size distributions for PSC layers at 15 and 19 km. The observed integral concentration points were obtained from 0.5 km averages. An air sample flow rate of 200 cm^3 s^{-1} and a nominal balloon

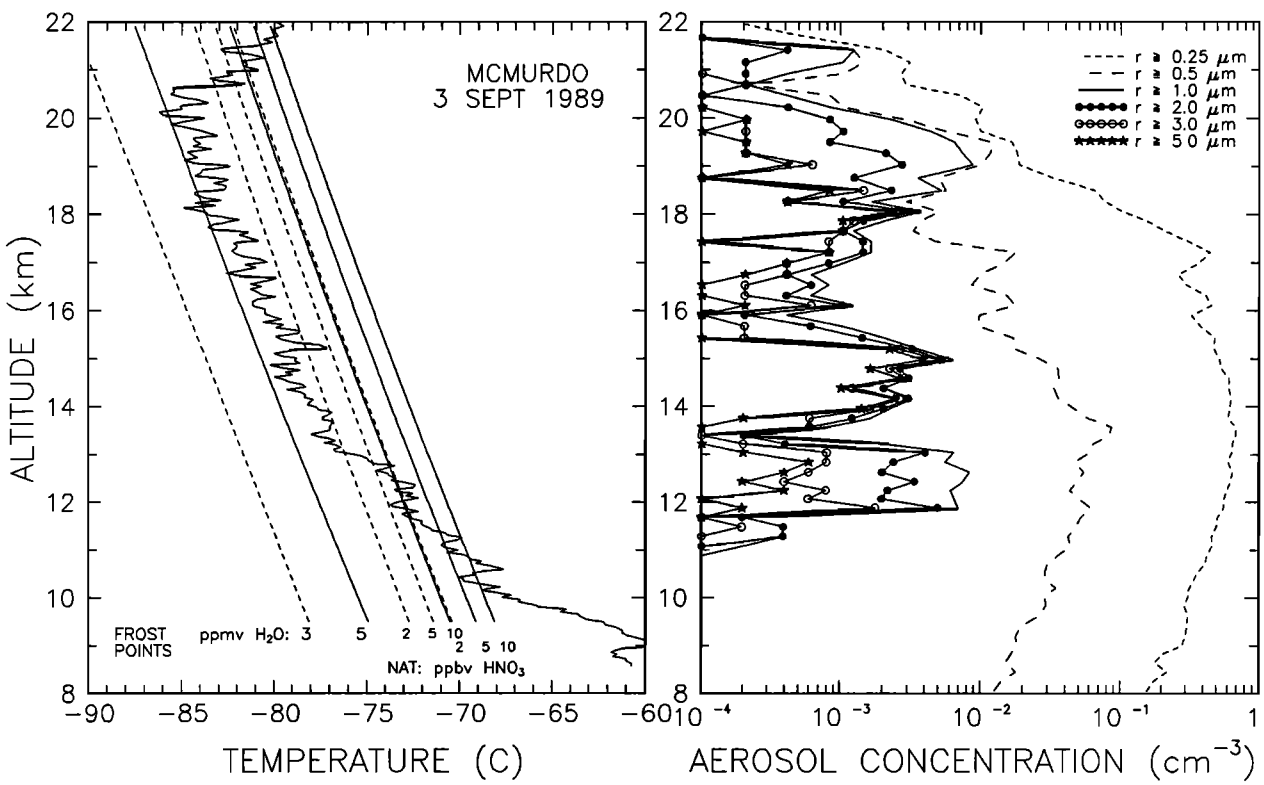

Fig. 9. Temperature and particle concentration profiles for several size ranges in the altitude region of PSC formation at McMurdo Station, Antarctica, on September 3, 1989. The smooth temperature curves are condensation temperatures for water ice and NAT for 3 ppmv H_2O vapor (dashed curves) and 5 ppmv H_2O vapor (solid curves) and several values of HNO_3 vapor mixing ratios as indicated in the figure.

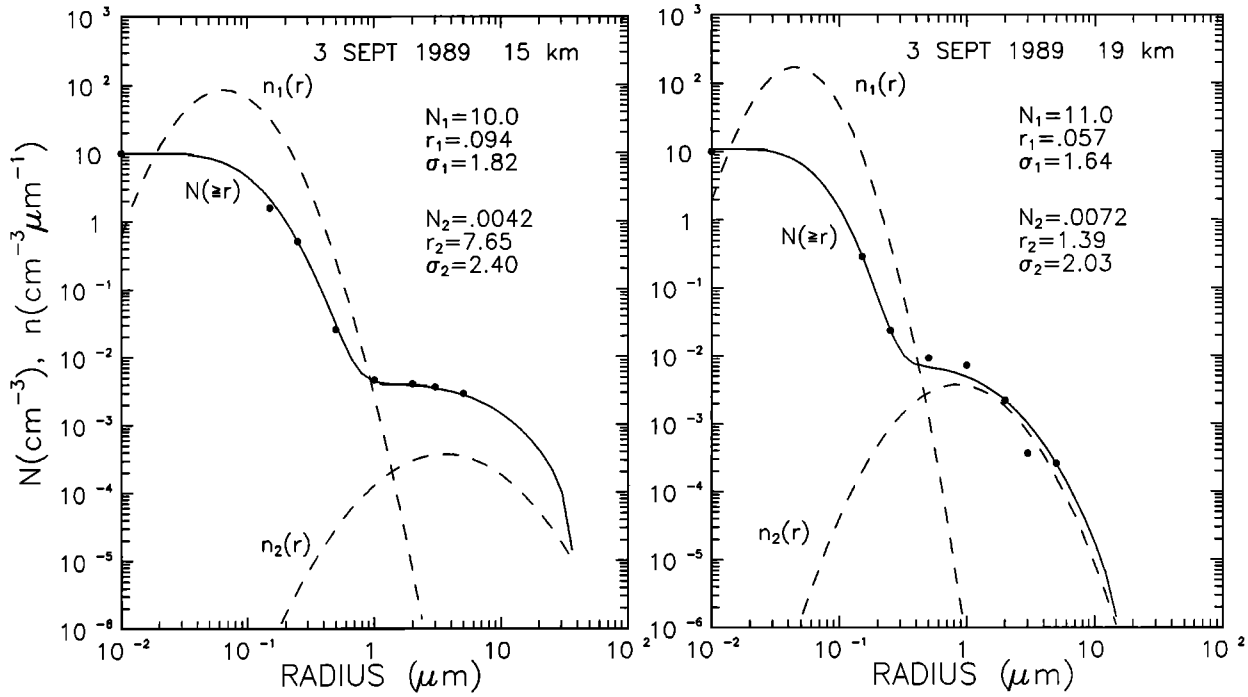

Fig. 10. Bimodal lognormal particle size distributions at 15 and 19 km altitude at McMurdo Station, Antarctica, on September 3, 1989. The measured points have been used to derive the differential distributions, n (dashed curves), which have been integrated to give the integral distribution, N (solid curve). Parameters of the lognormal distributions are given in the figure.

rise rate of 5 m s^{-1} amounts to a volume sample of 4 x 10^4 cm^3 km^{-1} or a statistical uncertainty of 0.71, 2.2, 7.1 and 22 % for 0.5 km average integral concentrations of 1, 10^{-1}, 10^{-2} and 10^{-3} cm^{-3}, respectively. For spherical or slightly nonspherical particles having radii smaller than about 0.5 μm the uncertainty in mass determinations of about 30%, owing to size uncertainties, exceeds the counting statistics uncertainty. With no knowledge of the shape of the larger particles, the uncertainty in particle volume again probably exceeds the counting statistics uncertainty even at the low concentrations involved and can result in large, indeterminable errors.

In addition to the observations of the integral concentrations, Figure 10 includes the optimum differential lognormal curves for the bimodal distributions, the derived mode parameters, and the integrated lognormal curve for comparison with observations. The parameters for these and other layers are given in Table 1. A layer at 18 km has a size distribution similar to the layer at 15 km (see Figure 9), and both are unusual since they contain relatively large concentrations of $r \geq 5$ μm particles. The large concentrations of these particles lead to uncertainties in determining the mode radius for the second mode and result in large mass errors. Nevertheless, it is clear that these layers cannot be made up entirely of NAT, but must be mainly water ice (see masses in Table 1). This suggests that the water vapor mixing ratio was at least 5 ppmv in these regions. The calculated mass in the layer at 19 km for an NAT composition gives an HNO_3 mixing ratio of about 3.6 ppbv in mode 2. Since the temperature is low enough to condense essentially all the available HNO_3 vapor at this altitude, the combined observations of mass and condensation temperature can be interpreted to indicate denitrification without substantial dehydration.

September 5, 1989. The vertical concentration profiles for this sounding are shown in Figure 11. Temperatures during this sounding were not as low as those on September 3. In the 10 to 20 km region the temperatures hovered around the 2 to 5 ppbv HNO_3 condensation curve for 3 ppmv H_2O. There was no evidence of ice crystal formation and inferred HNO_3 mixing ratios in the large particle mode were in the 1 to 3.5 ppbv range similar to those on September 3 in the absence of ice clouds (see Table 1). Although the PSC activity appears to cease at 18 km, in association with warmer temperatures in this region, particle data were not obtained above this altitude. Thus, the existence of enhanced large particles between 19 and 20 km, where temperatures decreased again below the 2 ppbv HNO_3 condensation temperature, could not be determined. The rather good correlation between enhanced large particle layers and temperature suggests that the HNO_3 mixing ratio profile was reasonably constant and the calculated HNO_3 vapor mass suggests that the water vapor mixing ratio was probably near 3 ppmv. The size dis-

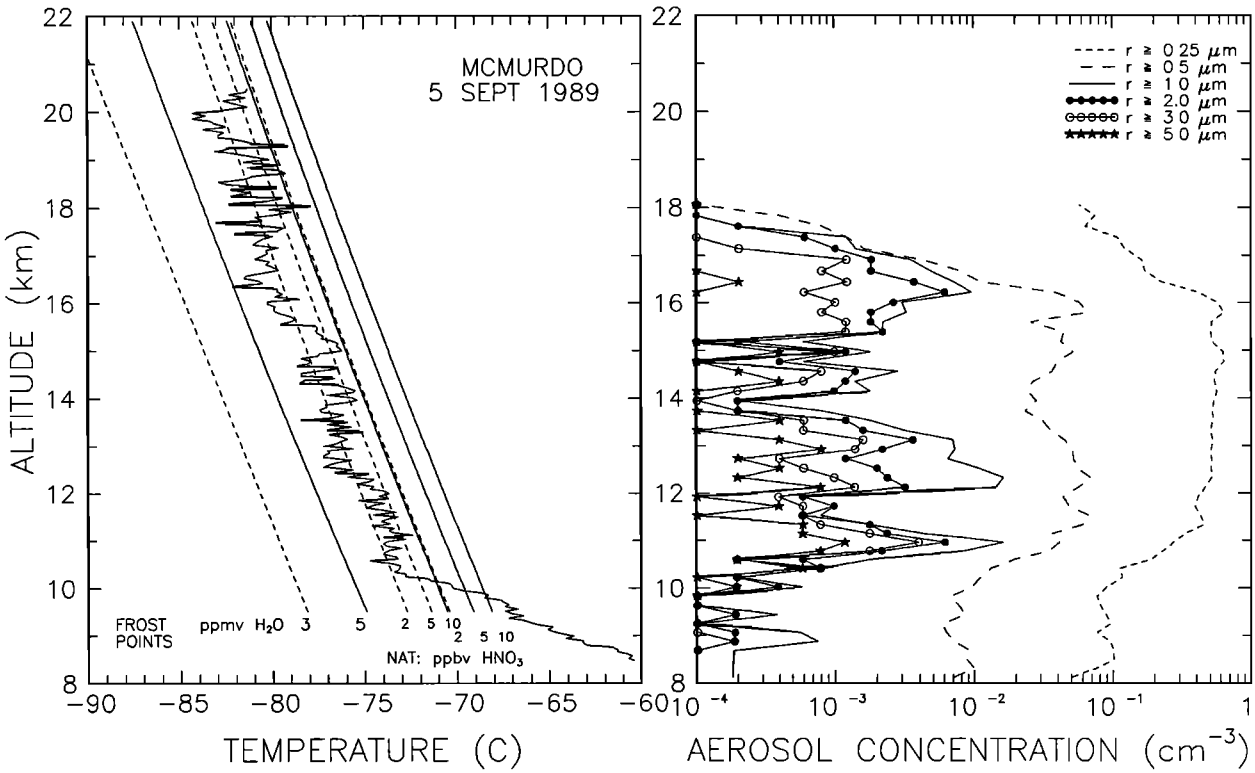

Fig. 11. Same as Figure 9 except for observations made on September 5, 1989.

tributions for layers at 13, 14.5, and 16.5 km in Figure 12 show a narrowing and increase in mode radius of the sulfate size distribution, $n_1(r)$, with increasing altitude, and also show the variability in the large particle, $n_2(r)$, NAT distributions.

September 10, 1989. Figure 13 shows the vertical concentration profiles for this sounding. Except for narrow regions between 13 and 14 km and 18 and 19 km, the temperatures were above the 2 ppbv HNO_3 condensation curve for 3 ppmv H_2O vapor. Only a few particles with radii greater than 1 μm were observed suggesting HNO_3 vapor mixing ratios of less than 5 to 10 ppbv. The temperature feature between 13 and 14 km is similar to those resulting from adiabatic vertical motions (potential temperature approximately constant with altitude) and may have been the result of recent mountain lee wave

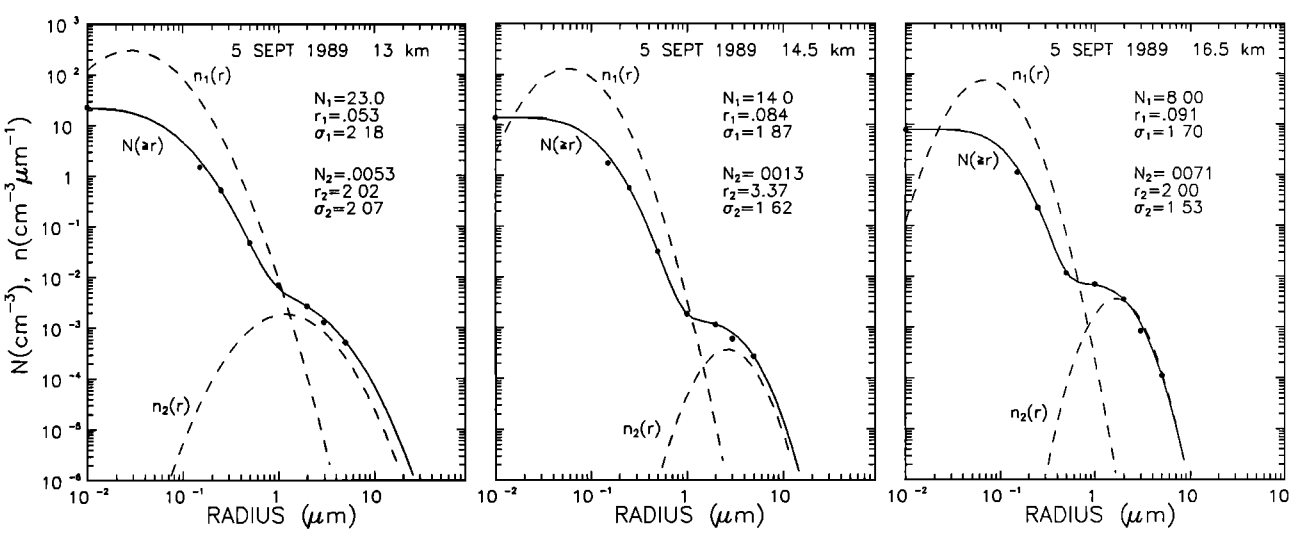

Fig. 12. Same as Figure 10 except for observations made at 13, 14.5, and 16.5 km on September 5, 1989.

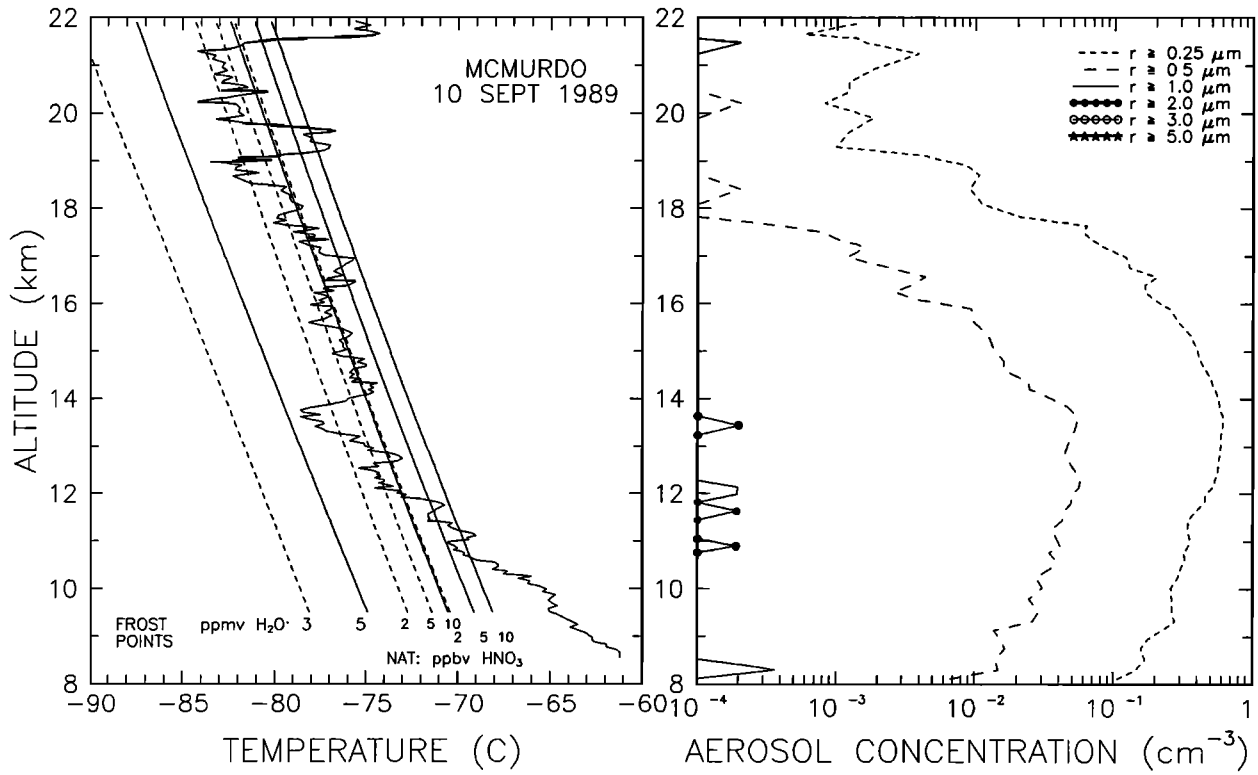

Fig. 13. Same as Figure 9 except for observations made on September 10, 1989.

activity which has been observed at McMurdo on other occasions [Hofmann et al., 1989a]. The fact that enhanced particle concentrations are absent in this region where condensation should have occurred for HNO_3 mixing ratios less than 2 ppbv, for 3 ppmv H_2O vapor, may be the result of the recent occurrence of the event. The size distribution at 13.5 km, shown in Figure 14, is clearly unimodal with parameters typical of the undisturbed sulfate layer.

September 18, 1989. Figure 15 shows the vertical concentration profiles for this sounding. Rather large particles were observed in the 10 to 12 km region. Water vapor mixing ratios would have to be in excess of 10 ppmv for these to be ice clouds. If these large particles are composed of NAT, then this observation suggests the redistribution of HNO_3 to lower altitudes by sedimentation. The calculated mass at 11.5 km (see Table 1) indicates about 9.5 ppbv HNO_3 vapor if composed of NAT, the largest value inferred for any cloud which did not appear to be composed of water ice. However, as the size distribution at 11.5 km in Figure 16 indicates, the large particle mode, with a mode radius of 5.28 μm, is not well determined and thus subject to considerable uncertainty. The observation of relatively more large NAT particles in the lower stratosphere is clearly indicated by comparison of the large particle modes, $n_2(r)$, at 11.5, 13.5 and 16 km in Figure 16. The settling velocity of 3 and 5 μm radius spherical particles in the stratosphere is 0.2 and 0.75 km day^{-1}, respectively, adequate for removal from the stratosphere in a period of less than 1 month.

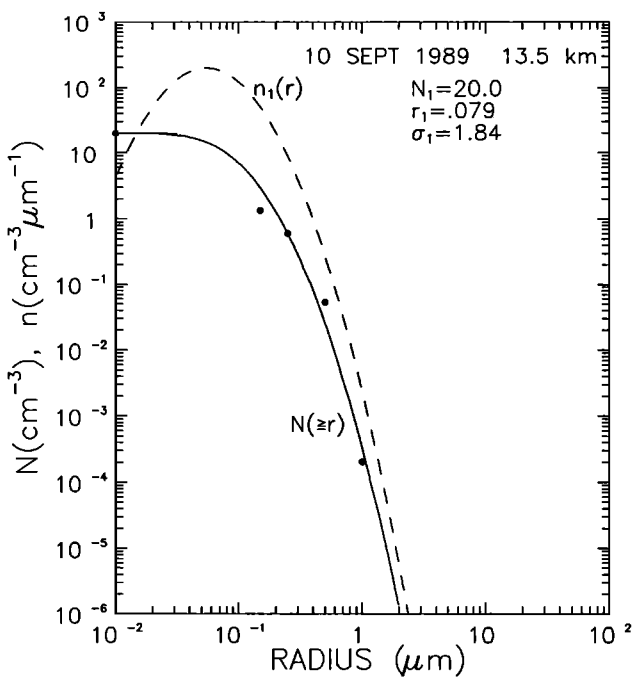

Fig. 14. Same as Figure 10 except for observations made at 13.5 km on September 10, 1989.

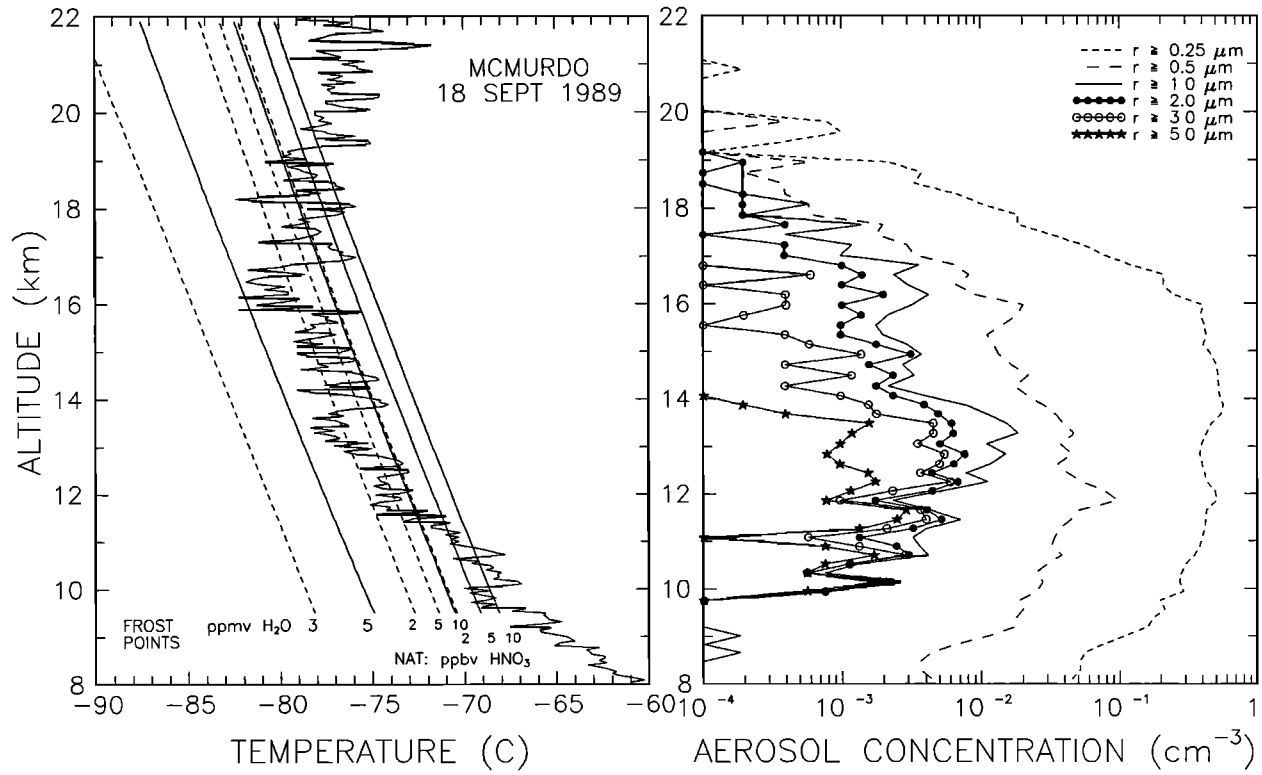

Fig. 15. Same as Figure 9 except for observations made on September 18, 1989.

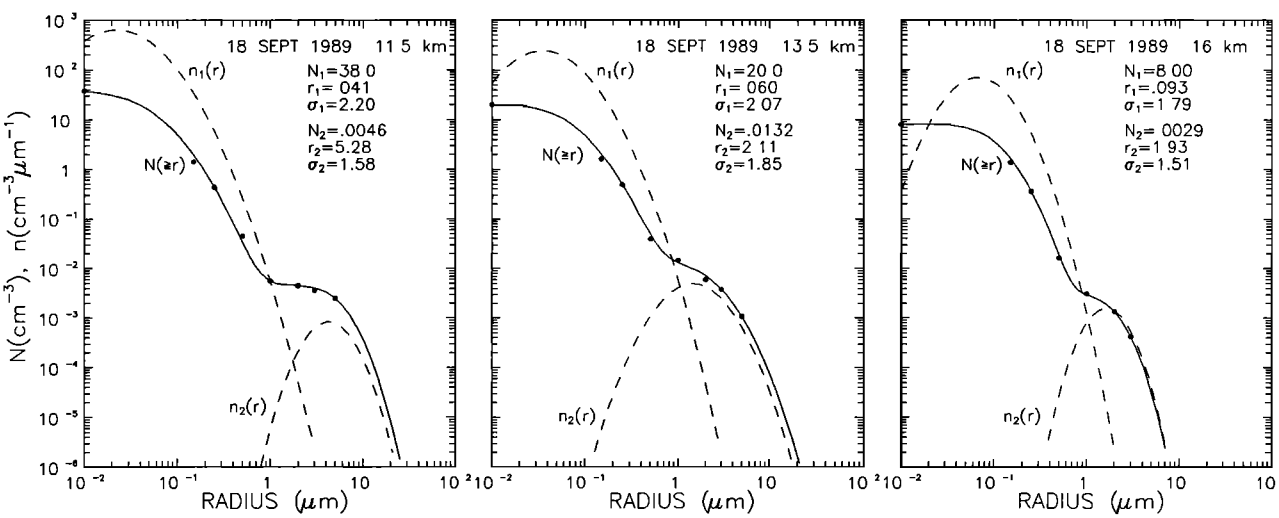

Fig. 16. Same as Figure 10 except for observations made at 11.5, 13.5, and 16 km on September 18, 1989.

September 20, 1989. Figure 17 shows the vertical concentration profiles for this sounding and indicates the most complicated temperature structure observed in any of the particle counter flights. Near constant potential temperature regions of 1 to 2 km extent occur throughout the 10 to 22 km region. This flight is typical of a high degree of mountain wave activity and was accompanied by elevated southerly winds over the Trans Antarctic Range. The small particle mode was enhanced, as discussed earlier and indicated in Figure 5, at the expense of the large particle mode which was underdeveloped at all altitudes, containing HNO_3 vapor masses of 1 ppbv or less (see Table 1). The region between 13 and 14 km reached ice condensation

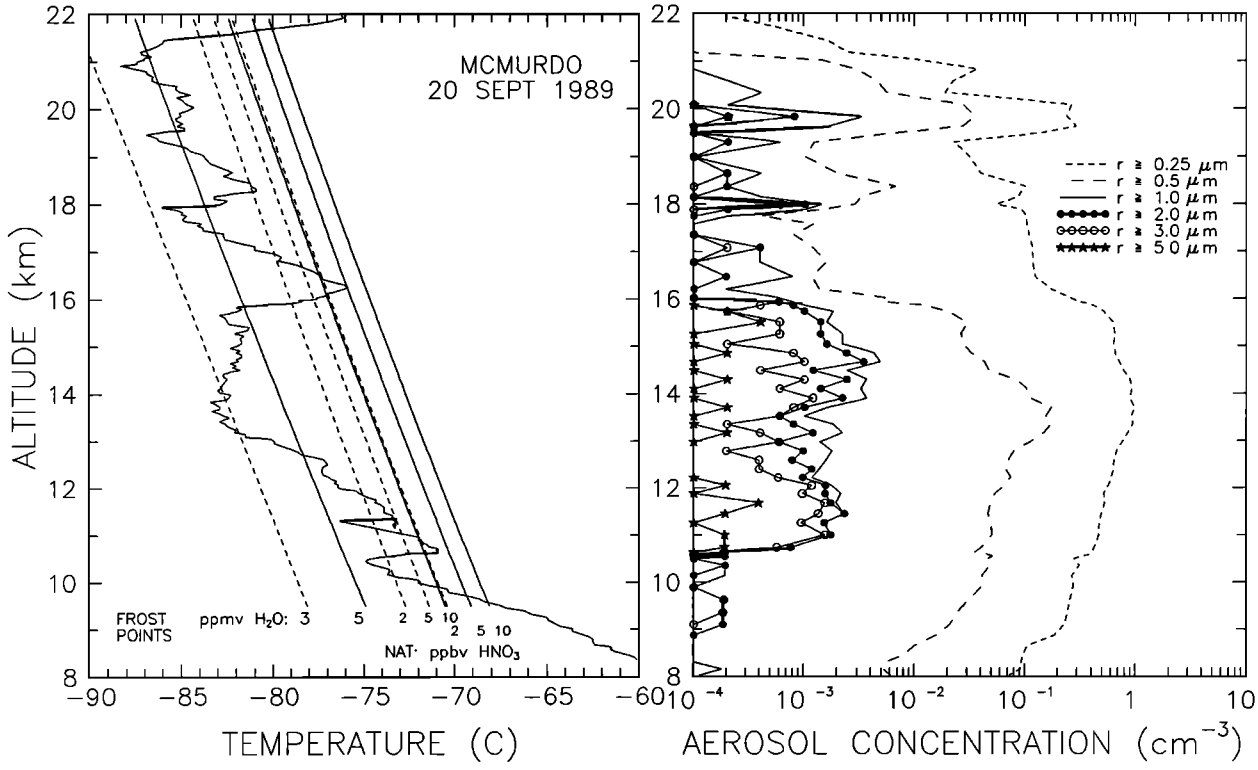

Fig. 17. Same as Figure 9 except for observations made on September 20, 1989.

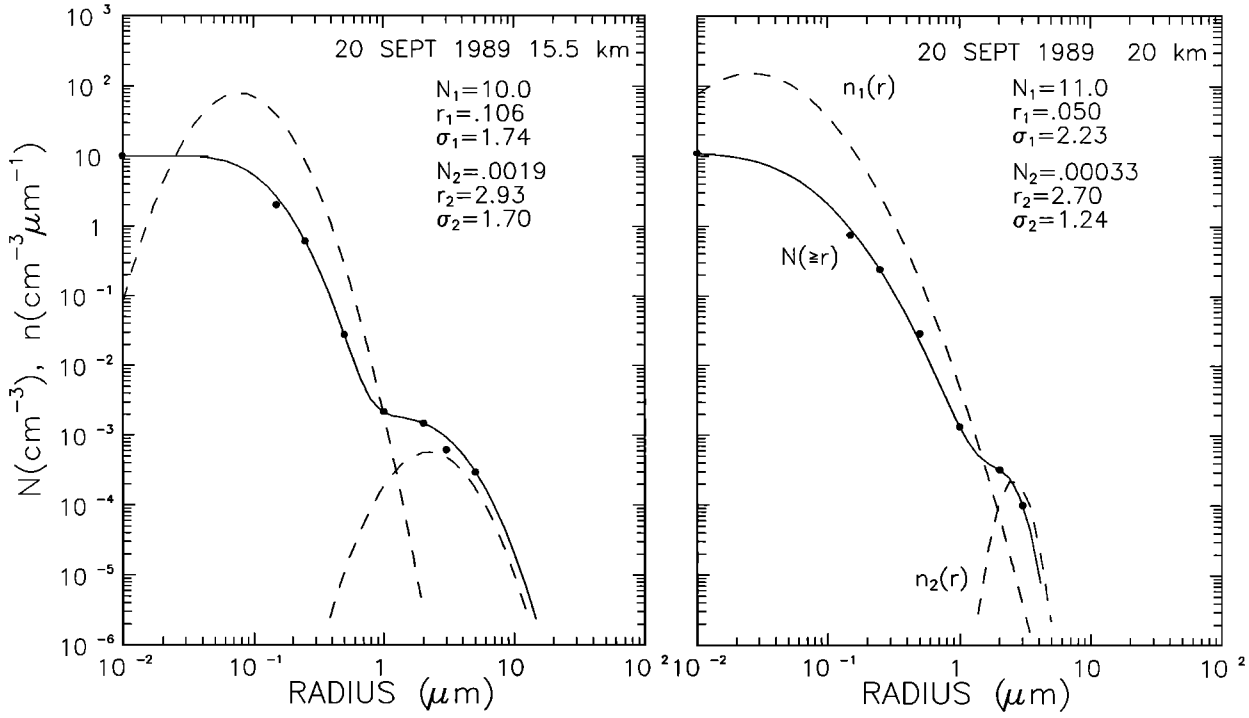

Fig. 18. Same as Figure 10 except for observations made at 15.5 and 20 km on September 20, 1989.

temperature for 3 ppmv H_2O; however, no large ice crystals were observed suggesting either substantial dehydration or that the event was related to local mountain wave activity and ice clouds had not had sufficient time to form. Size distributions at 15.5 and 20 km in Figure 18 show the weakness of mode 2 especially in the region of enhancement of mode 1 at 20 km.

Summary and Conclusions

Balloon flights with optical particle counters, covering the size range from $r \geq 0.15$ to 5 μm, and with condensation nuclei counters were used to characterize the PSC size distribution under varying temperature conditions at McMurdo Station, Antarctica, during the spring of 1989. A new particle counter, with size resolution in the 0.5 μm radius region, produced the most detailed size distributions of polar stratospheric clouds obtained to date. These data indicate that size distributions observed in the clouds were bimodal. Mode radii ranging from 0.05 to 0.10 μm were observed for the small particle mode, representing the sulfate layer or condensational growth enhancements of it. Mode radii generally ranged from 1.5 to 3.5 μm for the large particle mode at concentrations 3 to 4 orders of magnitude lower than the small particle mode. The large particle mode, believed to be the result of NAT condensation on larger particles of the sulfate layer, normally comprised most of the mass with inferred HNO_3 mixing ratios of 1 to 5 ppbv for most of the cloud layers observed suggesting varying degrees of denitrification.

Higher concentrations of large NAT particles in the lower stratosphere indicated the redistribution of HNO_3 through particle sedimentation. On several occasions, size distributions were observed with mode radii as high as 7 μm in the 12 to 15 km region, and, although the size distributions could not be accurately determined, large inferred masses indicated that they were probably the result of water ice formation. On other occasions, absence of ice clouds at very low temperatures indicated water vapor mixing ratios of less than 3 ppmv suggesting some degree of dehydration. On at least one occasion the data could be interpreted as suggesting denitrification without substantial dehydration (DWSD).

The possibility that DWSD can occur was predicted by Salawitch et al. [1989], based on the observation by Hofmann et al. [1989a], that under normal seasonal cooling rates, rather large ($r > 1$ μm) NAT particles form which may be subject to gravitational redistribution. Observations of DWSD in the Arctic in 1989 [Rosen et al., 1989; Kawa et al., 1990] support this contention. If temperatures are low enough, the large NAT particles may also preferentially accumulate water, grow still larger and fall without removing an appreciable amount of water. The formation of NAT particles as large as 1 μm is not expected on the basis of simple theories which tend to involve condensation on all available sites [Toon et al., 1986; Poole and McCormick, 1988a]. DWSD could also occur through the condensation of HNO_3 onto falling ice crystals, coating them with NAT and removing HNO_3 from the stratosphere [Wofsy et al., 1990]. Such a process would also be important in impeding the evaporation of large ice crystals. Observations of apparent large ice crystals in regions which are too warm for growth to occur [Hofmann and Deshler, 1989; Gandrud et al., 1990; Hofmann, 1990c] support this mechanism.

The preponderance of large NAT particles is clearly evident in the 1989 Antarctic data reported here. On the basis of comparative concentrations, all mode 2 particles appear to have been grown from sulfate aerosol having radii greater than about 0.3 to 0.5 μm, i.e., that less than 1 in 10^3 of the available condensation sites take part in the growth process, a fact surmised from earlier observations [Hofmann et al., 1989a]. However, there are occasions when numerous small particles form, at the expense of larger particles, under very cold conditions. It is likely that these colder temperatures resulted from recent fast cooling which caused condensation on a larger fraction of the available condensation sites.

Although the high flow particle counters were not available in 1987, when ozone depletion was as great or slightly greater than in 1989 and when dehydration and denitrification were the rule, comparisons with the low flow rate counters used in 1987 suggests that both of these phenomenon, important for ozone depletion, were not as prevalent in 1989. This supports the conclusion of Deshler et al. [1990], that 1989 presented conditions closer to the threshold required for maximum ozone depletion in the Antarctic spring than in 1987, while in the latter case these conditions were in excess of that required.

Acknowledgments. Assistance in Antarctica by J. Hereford, C. Sutter, and K. Harper and in the laboratory by G. Olson and S. Gabriel is gratefully acknowledged. This research was supported by the Division of Polar Programs, National Science Foundation.

References

Arnold, F., P. Metzinger, J. Hoffmann, H. Schlager, and S. Spreng, Stratospheric nitric acid condensation: Evidence from balloon and rocket measurements, *Nature*, *342*, 493-497, 1989.

Browell, E. V., C. F. Butler, S. Ismail, P.A. Robinette, A. F. Carter, N. S. Higdon, O. B. Toon, M. R. Schoeberl, and A. F. Tuck, Airborne lidar observations in the wintertime Arctic stratosphere: polar stratospheric clouds, *Geophys. Res. Lett.*, *17*, 385-388, 1990.

Crutzen, P. J., and F. Arnold, Nitric acid cloud formation in the cold Antarctic stratosphere: A major cause for the springtime "ozone hole," *Nature, 324*, 651-655, 1986.

Deshler, T., D. J. Hofmann, J. V. Hereford, and C. B. Sutter, Ozone and temperature profiles over McMurdo Station, Antarctica in the spring of 1989, *Geophys. Res. Lett., 17*, 151-154, 1990.

Fahey, D. W., K. K. Kelly, G. V. Ferry, L. R. Poole, J. C. Wilson, D. M. Murphy, M. Loewenstein, and K. R. Chan, In situ measurements of total reactive nitrogen, total water, and aerosol in a polar stratospheric cloud in the Antarctic, *J. Geophys. Res. 94*, 11,299-11,316, 1989.

Gandrud, B. W., P. D. Sperry, L. Sanford, K. K. Kelly, G. V. Ferry, and K. R. Chan, Filter measurement results from the airborne Antarctic ozone experiment, *J. Geophys. Res., 94*, 11,285-11,298, 1989.

Gandrud, B. W., J. E. Dye, D. Baumgardner, G. V. Ferry, M. Lowenstein, K. R. Chan, L. Sanford, B. Gary, and K. Kelly, The January 30, 1989 Arctic polar stratospheric clouds (PSC) event: Evidence for a mechanism of dehydration, *Geophys. Res. Lett., 17*, 457-460, 1990.

Hanson, D., and K. Mauersberger, Laboratory studies of the nitric acid trihydrate: Implications for the south polar stratosphere, *Geophys. Res. Lett., 15*, 855-858, 1988.

Hübler, G., D. W. Fahey, K. K. Kelly, D. D. Montzka, M. A. Carroll, A. F. Tuck, L. E. Heidt, W. H. Pollock, G. L. Gregory, and J. F. Vedder, Redistribution of reactive nitrogen in the lower Arctic stratosphere, *Geophys. Res. Lett., 17*, 453-456, 1990.

Hofmann, D. J., Direct ozone depletion in springtime Antarctic lower stratospheric clouds, *Nature, 337*, 447-449, 1989.

Hofmann, D. J., Measurement of the condensation nuclei profile to 31 km in the Arctic in January 1989 and comparisons with Antarctic measurements, *Geophys. Res. Lett., 17*, 357-360, 1990a.

Hofmann, D. J., Increase in the stratospheric background sulfuric acid aerosol in the past 10 years, *Science, 248*, 996-1000, 1990b.

Hofmann, D. J., Stratospheric cloud micro-layers and small-scale temperature variations in the Arctic in 1989, *Geophys. Res. Lett., 17*, 369-372, 1990c.

Hofmann, D. J., and T. Deshler, Comparison of stratospheric clouds in the Antarctic and the Arctic, *Geophys. Res. Lett., 16*, 1429-1432, 1989.

Hofmann, D. J., J. M. Rosen, T. J. Pepin, and R. G. Pinnick, Stratospheric aerosol measurements I: Time variations at northern midlatitudes, *J. Atmos. Sci., 32*, 1446-1456, 1975.

Hofmann, D. J., J. M. Rosen, and J. W. Harder, Aerosol measurements in the winter-spring Antarctic stratosphere, 1, Correlative measurements with ozone, *J. Geophys. Res., 93*, 665-676, 1988.

Hofmann, D. J., J. M. Rosen, J. W. Harder, and J. V. Hereford, Balloon-borne measurements of aerosol, condensation nuclei, and cloud particles in the stratosphere at McMurdo Station, Antarctica, during the spring of 1987, *J. Geophys. Res., 94*, 11,253-11,270, 1989a.

Hofmann, D. J., T. L. Deshler, P. Aimedieu, W. A. Matthews, P. V. Johnston, Y. Kondo, W. R. Sheldon, G. J. Byrne, and J. R. Benbrook, Stratospheric clouds and ozone depletion in the Arctic during January 1989, *Nature, 340*, 117-121, 1989b.

Kawa, S. R., D. W. Fahey, L. C. Anderson, M. Loewenstein, and K. R. Chan, Measurements of total reactive nitrogen during the Airborne Arctic Stratospheric Expedition, *Geophys. Res. Lett., 17*, 485-488, 1990.

Kelly, K. K., A. F. Tuck, D. M. Murphy, M. H. Profitt, D. W. Fahey, R. L. Jones, D. S. McKenna, M. Loewenstein, J. R. Podolske, S. E. Strahan, G. V. Ferry, K. R. Chan, J. F. Vedder, G. L. Gregory, W. D. Hypes, M. P. McCormick, E. V. Browell, and L. E. Heidt, Dehydration in the lower Antarctic stratosphere during late winter and early spring, 1987, *J. Geophys. Res., 94*, 11,317-11,358, 1989.

Kondo, Y., P. Aimedieu, W. A. Matthews, D. W. Fahey, D. G. Murcray, D. J. Hofmann, P. V. Johnston, Y. Iwasaka, A. Iwata, and W. R. Sheldon, Ballon-borne measurements of total reactive nitrogen, nitric acid, and aerosol in the cold Arctic stratosphere, *Geophys. Res. Lett., 17*, 437-440, 1990.

McCormick, M. P., C. R. Trepte, and M. C. Pitts, Persistence of polar stratospheric clouds in the southern polar region, *J. Geophys. Res., 94*, 11,241-11,252, 1989.

Poole, L. R., and M. P. McCormick, Polar stratospheric clouds and the Antarctic ozone hole, *J. Geophys. Res., 93*, 8423-8430, 1988a.

Poole, L. R., and M. P. McCormick, Airborne lidar observation of Arctic polar stratospheric clouds: Indications of two distinct growth modes, *Geophys. Res. Lett., 15*, 21-23, 1988b.

Pueschel, R. F., K. G. Snetsinger, J. K. Goodman, O. B. Toon, G. V. Ferry, V. R. Oberbeck, J. M. Livingston, S. Verma, W. Fong, W. L. Starr, and K. R. Chan, Condensed nitrate, sulfate, and chloride in Antarctic stratospheric aerosols, *J. Geophys. Res., 94*, 11,271-11,284, 1989.

Pueschel, R. F., K. G. Snetsinger, P. Hamill, J. K. Goodman, and M. P. McCormick, Nitric acid in polar stratospheric clouds: Similar temperature of nitric acid condensation and cloud formation, *Geophys. Res. Lett., 17*, 429-432, 1990.

Rosen, J. M., D. J. Hofmann, J. R. Carpenter, J. W. Harder, and S. J. Oltmans, Balloonborne Antarctic frost point measurements and their impact on polar stratospheric cloud theories, *Geophys. Res. Lett., 15*, 859-862, 1988.

Rosen, J. M., S. J. Oltmans, and W. F. Evans, Balloonborne observations of PSCs, frost point, ozone and nitric acid in the north polar vortex, *Geophys. Res. Lett.*, *16*, 791-794, 1989.

Salawitch, R. J., G. P. Gobbi, S. C. Wofsy, and M. B. McElroy, Denitrification in the Antarctic stratosphere, *Nature*, *339*, 525-527, 1989.

Schlager, H., and F. Arnold, Measurements of stratospheric gaseous nitric acid in the winter Arctic vortex using a novel rocketborne mass spectrometric method, *Geophys. Res. Lett.*, *17*, 433-436, 1990.

Solomon, S., The mystery of the Antarctic ozone "hole," *Rev. Geophys.*, *26*, 131-148, 1988.

Steele, H. M., and P. Hamill, Effects of temperature and humidity on the growth and optical properties of sulfuric acid-water droplets in the stratosphere, *J. Aerosol Sci.*, *12*, 517-528, 1981.

Steele, H. M., P. Hamill, M. P. McCormick, and T. J. Swissler, The formation of polar stratospheric clouds, *J. Atmos. Sci.*, *40*, 2055-2067, 1983.

Toon, O. B., P. Hamill, R. P. Turco, and J. Pinto, Condensation of HNO_3 and HCl in the winter polar stratosphere, *Geophys. Res. Lett.*, *13*, 1284-1287, 1986.

Toon, O. B., E. V. Browell, S. Kinne, and J. Jordan, An analysis of lidar observations of polar stratospheric clouds, *Geophys. Res. Lett.*, *17*, 393-396, 1990.

Tuck, A. F., R. T. Watson, E. P. Condon, J. J. Margitan, and O. B. Toon, The planning and execution of ER-2 and DC-8 aircraft flights over Antarctica, August and September 1987, *J. Geophys. Res.*, *94*, 11,181-11,222, 1989.

Turco, R., A. Plumb, and E. Condon, The Airborne Arctic Stratospheric Expedition: Prologue, *Geophys. Res. Lett.*, *17*, 313-316, 1990.

Wofsy, S. C., R. J. Salawitch, J. H. Yatteau, M. B. McElroy, B. W. Gandrud, J. E. Dye, and D. Baumgardner, Condensation of HNO_3 on falling ice particles: Mechanism for denitrification of the polar stratosphere, *Geophys. Res. Lett.*, *17*, 449-452, 1990.

T. Deshler and D. J. Hofmann, Department of Physics and Astronomy, University of Wyoming, Laramie, WY 82071.

(Received April 19, 1990;
revised October 29, 1990;
accepted November 9, 1990.)